Study of Insulator Flashovers caused by Atmospheric Ice Accumulation

M. Farzaneh **I. Fofana**
NSERC/Hydro-Quebec /UQAC Industrial Chair on Atmospheric Icing of Power Network Equipment (CIGELE) and Canada Research Chair, tier 1, on Engineering of Power Network Atmospheric Icing (INGIVRE)
Université du Québec à Chicoutimi, Québec, Canada G7H 2B1

Abstract - This paper summarizes the results of research recently carried out on the inception and propagation of electrical discharge on an ice surface. Investigations on discharge inception were performed using a simplified physical model consisting of a rod-plane gap half submerged in ice. Empirical models are proposed, based on elements derived from the inception parameter analysis, to account for corona streamer propagation velocity and inception voltage/field on an ice surface. Furthermore, a dynamic model is proposed to predict flashover of ice-covered insulators. Assuming arc behavior to be a time dependant impedance, it was possible to determine various arc characteristics, such as leakage current time histories and flashover voltage. The results indicate the feasibility of icing severity assessment and flashover prediction, using the proposed model.

Key words – insulators, atmospheric icing, corona streamer, leakage current, flashover voltage.

1. Introduction

During winter, power lines and communication towers can collapse as a result of freezing rain storms. The combined action of ice load and wind on power network structures is responsible for these failures. The most remarkable event of this nature during the last decade is certainly the famous January 1998 ice storm, when more than 85mm of freezing rain fell on Ottawa, 73mm on Kingston, 108mm on Cornwall, and 100mm on Montreal. As a result of this event, power network and telephone lines collapsed over a total length of 120,000km, depriving more than 900,000 households of electricity. Millions of people had to live in the dark for hours, days, or even weeks [1].

In addition to the phenomena leading to mechanical damages, the accumulation of ice or melting snow on outdoor insulators can also lead to a considerable reduction in their electrical performance. When combined with the aggravating factor of atmospheric pollution, ice or wet snow on insulators can induce corona discharges or partial arcs, leading to complete flashovers under certain conditions, and consequent power outages [e.g. 2-7], involving both line insulators and station post insulators.

Ice surface flashover has received much less attention than the phenomena leading to mechanical damages. Reviews of ice surface flashover literature [e.g. 2-7] indicate major lacks and the need for further research in this area, in order to be able to solve related practical problems. This is also necessary to establish powerful mathematical models able to account for the entire flashover development process. Understanding the fundamental causes of flashover on ice-covered insulators, such as electron avalanche formation conditions on an ice surface, is important for proper design of HV insulators destined to cold climate regions. In order to further our knowledge in this area, a research program has been initiated at the CIGELE and INGIVRE research chairs.

More precisely, the major objectives of this research are:

Furthering our knowledge of the inception and propagation conditions of discharges leading to flashover on ice-covered insulators.

Developing powerful mathematical models to predict the flashover process of ice-covered insulators.

The following fundamental investigations are necessary to meet these goals:

Theoretical study to represent the physical phenomena by mathematical models.

Setting the appropriate numerical methods to solve the proposed mathematical models.

Analysis and validation of the results with experimental data gathered under various conditions.

Such an approach is necessary to design insulators for cold regions.

In the first part of this paper, the investigations on streamer corona inception and propagation are summarized in a way which is accessible and useful to power engineers. The results are discussed and used to establish empirical models.

The second part is devoted to the mathematical modeling of the ice-covered insulator flashover process. The results from the model are compared to the minimum flashover voltages measured experimentally on a simplified physical model, as well as on a short string of five IEEE standard insulator units.

2. Insulator Icing and Flashover Processes

Flashover on an ice surface is an extremely complex phenomenon resulting from the interaction between the following factors: electric field, wet and polluted ice surface, presence of air gaps at the ice surface, environmental conditions, and the complex geometry of an ice-covered insulator [4].

To the best knowledge of the authors, there exists practically no exploratory research work providing an explanation of the mechanisms of flashover occurrence on ice-covered insulators. However, it is well established that several ice parameters, including type and density, amount and distribution, as well as the conductivity of freezing water forming the ice, have a significant influence on the flashover voltage of ice-covered insulators [2-15].

Natural atmospheric ice deposits on insulators generally result from a variety of conditions, including hoarfrost caused by condensation of vapor, in-cloud icing involving the freezing of super-cooled droplets in clouds or fog, and finally precipitation icing involving freezing rain, drizzle, or wet snow.

Ice deposits may be produced following a dry or wet regime [4, 5, 7, 9]. The ice grown is referred to as a dry regime when the ice deposit temperature remains below 0°C. On the other hand, it is referred to as a wet regime when the deposit temperature is 0°C.

The density of ice accretions depends on several major parameters, such as the median volume of droplets and their impact velocity, as well as the deposit temperature. Dry ice accretion is called hard or soft rime according to its physical appearance and density, as described in Table 1 [7, 9]. In a wet regime, the accreted ice is called glaze. Icicles are formed when the flux of water is high enough. Glaze with icicles is known as the most dangerous type of ice associated with a high probability of flashover on insulators [4, 5, 7, 9].

TABLE 1: CHARACTERISTICS OF ICE FORMED ON STRUCTURES [7, 9].

Type of ice	Density (g/cm^3)	Appearance	*Shape*
Glaze	0.8 – 0.9	Transparent and clear	Cylindrical icicles
Hard rime	0.6 – 0.9	Opaque	Eccentric pennants into the wind
Soft rime	< 0.6	White and opaque	Feathery and granular

The amount of ice accumulated, the number of icicles, and ice thickness layer all have a considerable effect on the withstand voltage. In general, when ice thickness increases, the maximum withstand voltage, V_{ws}, decreases [4, 5, 7, 9, 16]. However, it seems that the V_{ws} levels off after complete icicle bridging is reached [4, 5, 7, 9].

As concerns ice distribution along insulators, it should be noted that, in general, during icing events, only the windward face of the insulator is covered with ice and icicles, while the opposite side is free of ice. Ice uniformity is affected by wind velocity during ice accretion [7, 9]. For higher wind velocities, icicles were tilted away from the wind. Experimental laboratory results showed that the lowest values of V_{ws} for various insulators tested corresponded to the vertical icicles formed at a low wind velocity [7, 9]. Also, ice accretion along insulators is not uniform, as several parts of the insulators are free of ice; these zones are referred to as air gaps. Air gaps are caused by ice building and shedding during or after ice accretion. This is due to the heating effect of partial arc activity, increase in air temperature, or ice shedding.

It is generally agreed that the presence of a water film on the surface of the ice is necessary for flashover to occur [4, 5]. The water film on the ice surface may be caused by sunshine, a rise in air temperature, condensation, electrical discharge on ice particles, or by leakage current at the ice surface [4, 5, 13, 14]. Water film is highly conductive, sometimes ten times as much as freezing water [13, 14], due to the fact that, during the solidification process of the super-cooled droplets, the impurities tend to transfer from the solid to the liquid part. Moreover, the water film is

polluted by products of corona discharge. Under such conditions, voltage drop is predictably high across the air gaps (Figure 1) [17].

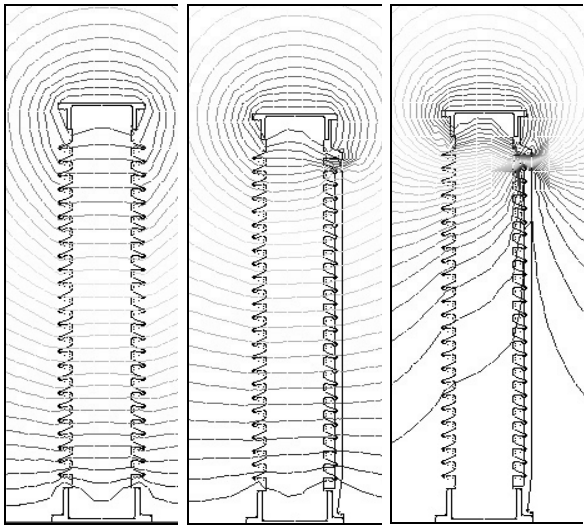

Figure 1: Potential distribution for a clean insulator. Equivalent potential curve separation: 3.125%. **(a)** Clean insulator, **(b)**: Ice layer with upper air gap and **(c)**: Ice layer covered with water film with upper airgap.

If the electric field across air gaps is high enough, corona discharges are initiated. This can lead to the development of local arcs across the air gaps (Figure 2) causing a substantial increase in leakage current and a concomitant melting of ice. If the electrical current circulating through an arc is interrupted (AC arcs), the plasma does not disappear instantly because the time constants for plasma decay are, in general, not negligible at the scale of the other durations involved in the phenomenon [18]. The relevant plasma is termed “afterglow”. As a rule, exact knowledge of the behavior of afterglow plasma is important in order to determine the possible conditions of either direct or inverse re-ignition.

Under sufficient electrical stress, local arcs propagate along the ice surface, forming a white arc, possibly bringing the insulator to flashover when it reaches a critical length.

Freezing water conductivity, which plays an important role in the flashover process, significantly influences the V_{ws} of ice-covered insulators [4, 5, 10-12]. In general, an increase in conductivity leads to lower flashover voltages.

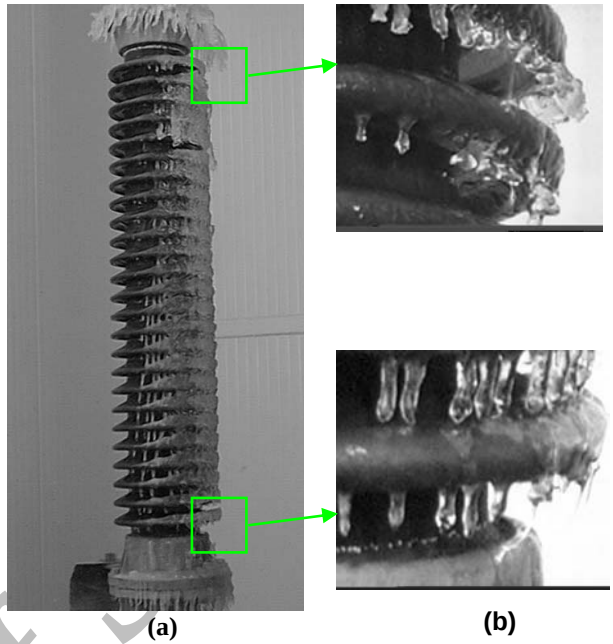

Figure 2: Corona discharge along the air gap. **(a):** ice-covered post-station insulator with air gaps; **(b):** inception of corona discharge along the air gaps. Corona streamer on an ice surface

3.1. Streamer Inception

Corona inception is known to be a statistical event [19-27]. Basically, three conditions must be met to obtain streamer inception: (i) an initial electron, (ii) applied field above the so-called critical field strength, E_{cr}, and (iii) sufficient or critical volume characterized by the critical distance, X_{cr} (Figure 3).

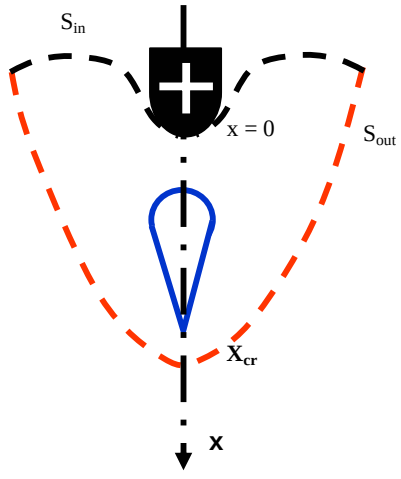

Figure 3: Representation of the critical volume in a positive discharge sequence.

It is supposed that a few electrons are always around in the interval between electrodes, either by the action of cosmic rays, from natural ionization sources,

residual charges from previous discharges, or else as a consequence of field emission from asperities on the surface, close to which electric fields are strongly enhanced [23, 24, 27]. To initiate critical size avalanches, one of these electrons must be suitably situated, i.e. in the so-called 'critical volume'. The critical volume is the volume of gas surrounding the high-voltage electrode, within which critical avalanches can develop sufficiently to lead to the development of a streamer (Figure 3). This volume is characterized by two boundaries defined by two limits, S_{int} and S_{ext}, of this critical volume:

$$S_{in} \quad : \quad x=0 \quad \text{and} \quad \exp \int_{x_{in}}^{x_0} (\alpha - \eta) dx \geq 10^8 \qquad (1)$$

$$S_{out} \quad : \quad X = X_{cr} \quad \text{and} \quad E = E_{cr} \qquad (2)$$

The critical field E_{cr} depends on the rod radius and relative air density [23, 24, 27].

3.2. Form Factor

In calculating electric field distribution and maximum field strength, parameters such as form factor and geometry, are generally used. The form factor, F, of a non-uniform field electrode configuration is defined as:

$$F = E_{mean} / E_{max} \qquad (3)$$

where E_{mean} is the average field strength of the arrangement over the electrode spacing, usually designated as the gap length, and E_{max} is the highest field strength appearing in the field region.

3.3. Physical Model and Facilities

The physical model used for streamer inception and propagation on the ice surface consists of a rod-plane gap configuration half-submerged in the ice bulk (Figure 4), where the inter-electrode distance, d, is adjustable. For the purpose of this study, rods with various radii (1.5, 3, 6 and 9 mm), and a fixed inter-electrode distance of 35 mm were used. The electrodes were screwed into a rectangular Plexiglas box, which also served as a mould to form the ice [28-31].

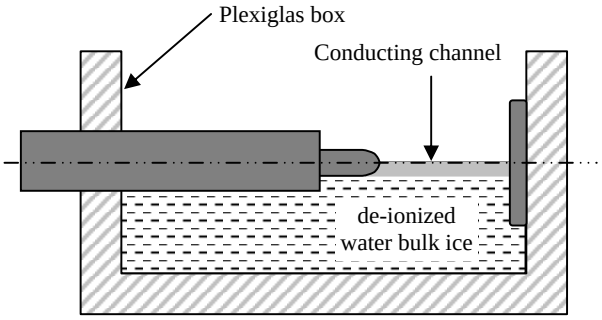

Figure 4: Vertical section of the physical ice model.

Figure 5 shows the experimental set up which consists of an HV impulse generator, a streak camera, and a cold chamber containing the physical model. Details of this experimental set-up and the ice mass of the built-up test specimen may be found in our previous papers [28-31].

A standard 1.2/50 μs positive lightning impulse voltage was applied to the rod to stress the inter-electrode distance through an HV impulse generator. The streak sweep duration of the camera used to record the optical phenomena can be varied from 0.5ns to 1ms. The wavelength covered by the camera ranges from ultraviolet light to the near infrared region (200 to 850 nm).

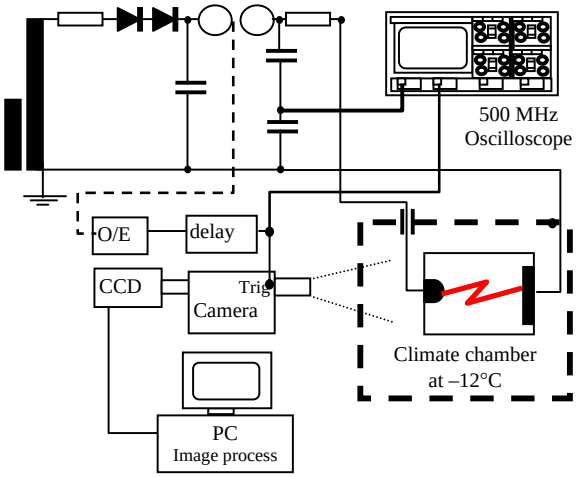

Figure 5: Schematic diagram for the HV circuit and streak camera.

3.4. Results and discussion

]In addition to the ice surface, the corona discharge was also studied in the ice-free space between the electrodes (air gap). This will be referred to as the air reference case.

Various parameters were obtained using streak camera recordings, such as voltage, time to develop

the first corona, and axial velocity of the streamers propagating between the electrodes. The first corona was quantitatively assessed through the inception voltage U_{inc}. As for the time to develop the first corona (T_{inc}) at the HV electrode, it was obtained from the time delay between the start of the pulse voltage waveforms and the first appearance of light, as detected by the camera.

Typical experimental results in the form of streak recordings are presented in Figures 6 and 7, for ice and air reference respectively.

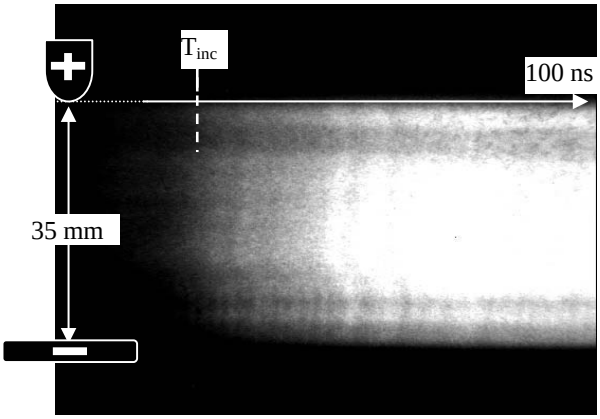

Figure 6: Typical recordings of corona inception and propagation on an ice surface.

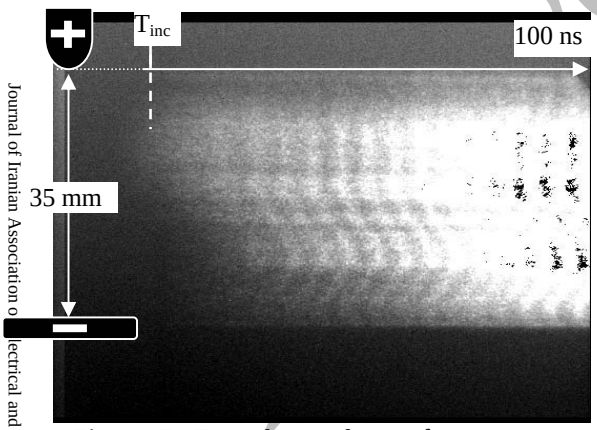

Figure 7: Typical recordings of corona inception and propagation in the air gap.

These streak images were recorded with a sweep period of 100ns. The vertical axis in the photographs is aligned with the axis of the electrodes, whereas the horizontal axis represents time. From these Figures, it may be observed that the discharge is initiated at the high-voltage electrode and gradually develops to reach the ground electrode (cathode). It may be observed that the discharge propagation velocity is faster for the ice surface than for the air gap.

3.4.1. Critical volume

In our previous investigations [28, 30], where a system with two active electrodes was used, it was established that the critical volume decreases substantially in the presence of an ice surface, as compared to the case of air. In the present study, similar investigations were carried out using the physical model presented in Figure 4. In this case, only one active electrode is considered while varying the radius of the HV rod electrode and the freezing water conductivity, σ, of the conducting channel (Figure 4). Figure 8 presents the axial distance from the critical volume according to the model.

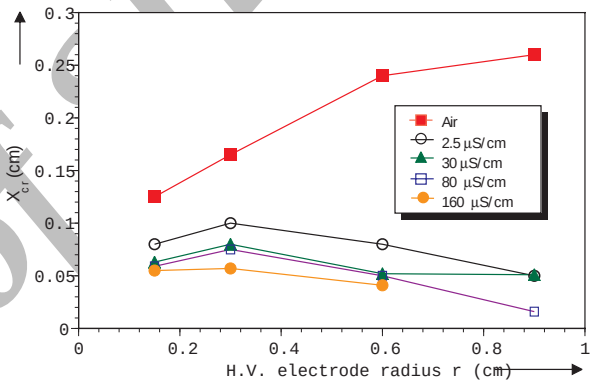

Figure 8: The critical distance for various electrode radii in the case of air and in the presence of an ice surface formed with freezing water of various conductivities.

It can be seen that the critical distance, X_{cr}, in the presence of an ice surface is reduced, because the high permittivity of ice (~75) draws in the line of force from the electrodes, making the field very high near the electrodes but weaker away from them. This therefore indicates that, for a given voltage applied to the electrode, the probability of finding an electron in a smaller critical volume is reduced in the presence of ice and, consequently, the voltage required to initiate a corona at a given time should be higher. This is in agreement with the results obtained with a two active electrode configuration, as well as those obtained by Allen et al. [20], who performed a comparative study between critical distances in air and on insulating material surfaces.

The higher is the conductivity (σ) used to form the conducting channel, the lower is the critical distance. This finding can be explained by the fact that, contrary to the critical field, which depends only on the size of the high voltage rod electrode and on air density [23, 24, 27], the corona streamer inception field

additionally depends on σ. By increasing the conductivity, σ, the discharge is initiated at lower voltages, which leads to a decrease in the inception field and, consequently, to a decrease of the critical distance X_{cr}. Because the impurities rejected into the ice surface during the freezing process are non-volatile and insoluble in ice, small amounts of impurities contained within the ice will increase the surface conductivity and decrease the activation energy [32-34]. Moreover, experimental evidence has revealed the presence of a liquid-like layer, or pre-melting layer, at the surface of ice at temperatures below the bulk melting transition [32]. Its thickness ranges from 0.3 to 17 nm for temperatures varying from –28°C to -0.02°C [32]. This liquid or liquid-like film is an electrolyte solution containing, for example, a monovalent ionic species such as NaCl. Among the various atoms and molecules that may be found on the surface of ice, NaCl and other Na derived ions almost have the lowest ionization energy [25, 34, 35].

The results also show that in the air, the critical distance increases with an increase in the rod radius, whereas on an ice surface, it reaches the maximum for a rod electrode of a radius of 3mm. This value is curiously close to the icicle radius accumulated on a structure, which is equal to 2.5mm [36]. Similarly with discharge observations in air [27], the concept of a critical radius may be introduced. The critical radius, which depends only on the gap spacing and electrode radius, is defined as a radius above which the breakdown probability increases. The decrease in the critical distance for radii higher than 3mm could be related to this concept. Additional investigations considering different gap spacings are necessary to draw more general conclusions.

3.4.2. Corona inception electric field

Knowing the development time of the first corona, T_{inc}, allows to determine the inception voltage, U_{inc}, from the voltage wave shape recorded by the oscilloscope. The inception time and time to breakdown were measured from oscillograms. The average value and standard deviation of these two parameters were calculated from a set of 10 shots.

The inception field E_{inc} was calculated using geometric field plots from Coulomb 3D, integrated engineering software using a method described in [28-31]. In previous studies [31], field computation resulting from this software was compared to analytical ones. The good correlation between both approaches supports the reliability of the geometric field plot method for assessing the electric field at the HV electrode in the absence of surface space charges.

The results of the maximum electric field, E_{max}, between the electrodes of the physical model presented in Figure 4, using Coulomb 3D, are summarized in Table 2.

Table 2: Form factor F for various electrode radii.

r (cm)	0.15	0.3	0.6	0.9
E_{max} (V/cm)	2.59	1.71	1.08	0.86
F	0.11	0.17	0.27	0.33

Figure 9 illustrates the inception electric field, E_{inc}, for different values of F, as a function of freezing water conductivity, σ.

A mathematical approach to process the data reveals a relationship between the inception field, E_{inc}, the form factor, F, and freezing water conductivity, σ:

$$E_{inc} = [-61\ln(F) + 450]\exp(-8.310^{-4}\ \sigma) \quad (4)$$

where E_{inc} and σ (measured at 20°C) are expressed in kV/cm, and μS/cm respectively.

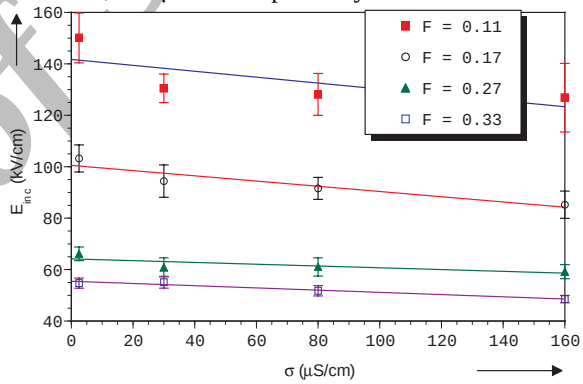

Figure 9: Corona inception field on the ice surface as a function of freezing water conductivity for different form factor.

It should be pointed out that equation (4) is valid under the experimental conditions tested in the present study but could be extended to other conditions.

3.4.3. Corona average propagation velocity

One important feature, essential to understanding how a streamer corona and an ice surface interact, is the velocity of the streamer when it propagates along the surface. Both the corona streamer transit time between electrodes and the average propagation velocities of the streamers were determined using the streak images recorded by the high-speed camera. Typical streamer mean velocities for air and ice surfaces as a function of inception voltage, U_{inc}, are shown in Figure 10. Each point represents an average value of 10 measurements.

Streamer propagation velocities in air are of the

same order as those reported elsewhere [24]. The propagation velocity is of the order of 10^6 m/s, which noticeably exceeds the speed of the electrons ($\cong 10^5$ m/s) [24]. The results show that the streamer propagation velocity on an ice surface is higher than in air, as seen in the streak recordings on Figures 6 and 7.

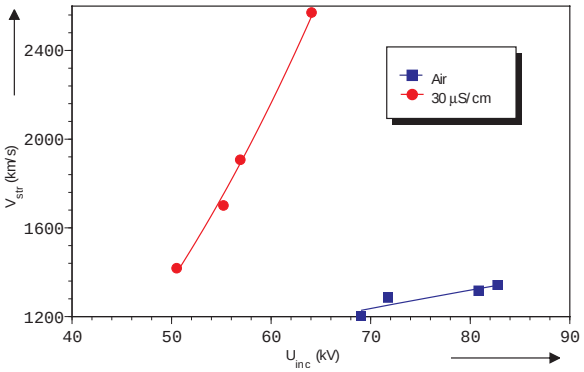

Figure 10: Streamer mean propagation velocity in air and on an ice surface, as a function of the inception voltage U_{inc}.

The presence of an 'insulator surface' clearly interacts with the discharge process, making it different from the discharge observed in air gaps alone, and thus remarkably affects the dielectric strength [e.g. 19-22, 37, 38]. The major difference between a breakdown in a pure gas and one at or near a dielectric surface is the change in the ionization growth rate coefficients [21, 22]. This variation is attributed to the change in ionization coefficient and/or the transport parameters that are in turn affected by a wide number of other parameters [21].

In Figure 10, it can be observed that the streamer mean propagation velocity increases with an increase in inception voltage U_{inc}. This finding is in agreement with observations from Chiba *et al.* [39], who found that streamer propagation velocity is controlled by many factors, including the capacitance of inter-electrode spacing, the shape of the electrodes, and the inductance of the circuit. In the present study, however, the presence of an ice layer between the electrodes modifies the spacing capacitance.

Several factors may affect the speed of streamer propagation on an ice surface. The most direct explanation would be the electric field enhancement caused by permittivity [19, 30]. Since ionization rate is a function of the local electric field, any enhancement of the field at the tip of the streamer will increase the coefficient rate.

There could also be other contributing factors, like the ones that add to or cancel the effect of permittivity, e.g. the charge accumulated on the ice surface. The presence of excess ions on the surface will increase the charge injected and the mean radius of the corona, both attributable to increased streamer discharges. Specific investigations have shown that the most important effect of excess ions on a surface is to provide 'seed' electrons for streamer propagation, following ion detachment in the field of advancing streamer tips [19, 30].

Another possible physical mechanism that could add to the effect of the accumulated surface charge is the release of electrons from the ice surface due to various mechanisms, including photo-ionization. The lowest energy required to remove an electron from a solid is called the work function ($e\phi$). This energy can occur in various forms: thermal (phonons, kT), photons ($h\nu$), internal potential energy of the atoms and ions (eV^*, eV_i), and kinetic energy ($\frac{1}{2}Mv^2$). From the range of atoms and molecules that may be found at the head of the streamer, NaCl and derived Na ions practically have the lowest ionization energy [25, 34, 35]. Avalanche growth and streamer propagation on an ice surface could therefore be controlled by increasing the ionization coefficient. Increased ice surface conductivity could also lead to a much faster streamer development.

The propagation velocity, V_{str}, is known to be a power function of the electric field [40-42]. It can therefore be expressed accurately in terms of the inception voltage U_{inc} (Figure 10), as follows:

$$V_{str} = a\, U_{inc}^{b} \qquad (5)$$

where the constants a and b, depending on the discharge propagation support, are presented in Table 3.

This relationship makes it possible to predict the streamer propagation velocity on an ice surface or in air. It is valid under the experimental conditions tested, but could be extended to other conditions.

Table 3: Parameters *a* and *b* for air and ice surface.

	Air	Ice surface (σ = 30 µS/cm)
a ($km.s^{-1}$)	164	0.067
b	0.49	2.53

4. Dynamic Modeling of Iced Insulator Flashover Characteristics

Results of previous work in DC arc propagation on an ice surface [43] are in good agreement with experimental results obtained using a simplified physical model, as well as one using real insulators. To the best of our knowledge, this is the first time a dynamic model is proposed for predicting flashover processes on ice-covered insulators. However, it is agreed that any such model must be handled differently, whether it is used in DC or AC. Indeed,

comparative tests based on power supply units cast any doubt as to the fundamental role played by the zero passages of the current when tested under alternating voltages. A self-consistent dynamic model to determine AC arc characteristics, as well as the minimum flashover voltage on an ice surface, is presented below.

4.1. General description of the modeling

Figure 11 shows a simplified flowchart of the self-consistent time-dependent mathematical model.

The model takes into account the instantaneous changes of the arc parameters, the time lag to flashover, the arc propagation velocity, as well as the surface conductivity of the ice layer.

The input data are the insulator geometry, ice layer characteristics and/or properties, applied voltage, and some initial values. The discharge time base is divided into steps d*t*, starting from $t = 0$.

Under the estimated flashover voltage, which should be enough to sustain an arc beyond the first arc length, the arc development begins when the propagation criterion is met. The internal conditions (velocity, radius, electrical parameters, etc.), as well as the residual ice layer resistance, are calculated. Under AC, the applied voltage, $V_{ap}(t)$, is calculated at each time step. To calculate the flashover voltage (FOV), the same hypothesis as for static modeling [15, 44] is assumed, i.e. the flashover takes place during a short period of time around the peak value of applied voltage [45].

At each time step *dt*, the critical conditions for continued propagation of the discharge are tested and, if they are satisfied, the discharge will continue to progress up to the final jump stage. Otherwise, the arc will extinguish and flashover will not take place. Then, a new step is considered by increasing the applied voltage. The simulation is restarted again with initialization of the input data. At the time the arc length x becomes equal to the insulator length L_f, flashover takes place. Under AC voltage, this moment happens at the peak value of the last quarter cycle (T/4, T being the period) [45] and so, velocity is adjusted to achieve a total flashover at this time.

Before this moment, while the surface conductivity is less than its critical value, the length of arc is considered constant and the current variation is due to the surface conductivity change, as well as to the arc resistance. Then, under the calculated value of flashover voltage, the simulation is repeated to calculate the parameters in the last stage. During each iteration, arc resistance and length are initialized.

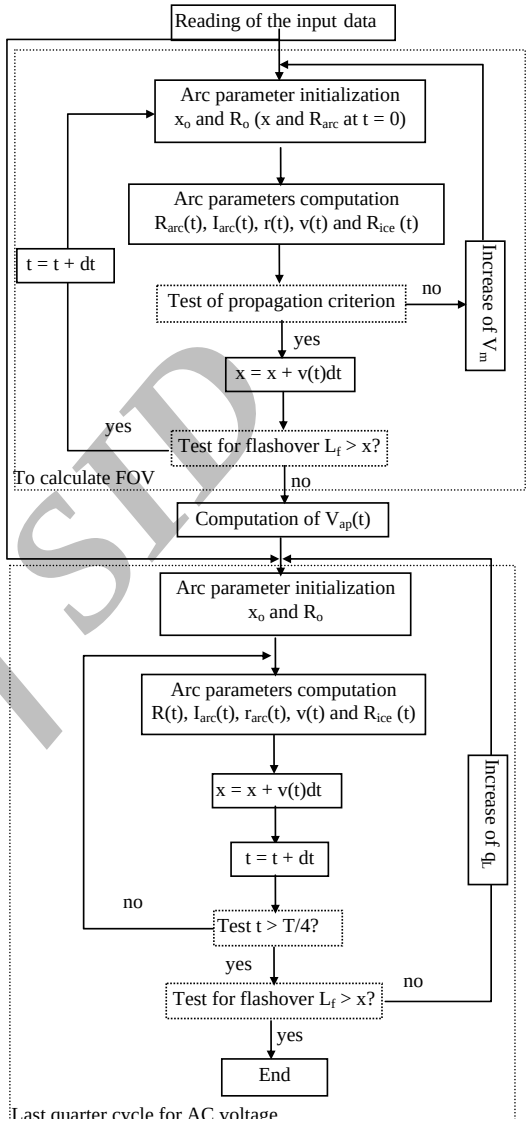

Figure 11: General flow-chart of the modeling.

4.2. Mathematical modeling

One of the first quantitative analyses of arcs on contaminated surfaces was carried out by Obenaus in 1958 [46]. So far, the most practical and useful models proposed by other authors have been based on the well-known design, where a polluted insulator is represented by a simple electrical equivalent circuit consisting of an arc in series with an electrical resistance. The air gaps on ice-covered insulators (or parts of the insulators free of ice) in series with the accumulated ice, and which have a relatively high surface conductivity, present situations similar to the dry bands in series with the wet part of insulators, in the case of polluted surfaces. Thus, a comparable

model can be used [44].

In the present study, the arc channel is assumed to be cylindrical with a radius r and length x, and is represented by a RLC electrical network (see Figure 12). The model is self-consistent and time-dependant; its input data are applied voltage characteristics, ice-covered insulator geometry, and characteristics.

When the arc propagates, the potential wave and current initiated are described by:

$$V_{ap}(t) - V_c(t) = R_{arc} I_{arc}(t) + L\frac{dI_{arc}(t)}{dt} \quad (6)$$

and

$$I_{arc}(t) = C\frac{dV_c(t)}{dt} - \frac{1}{R_{ice}}V_c(t) \quad (7)$$

where V_c and I_{arc} are the potential across capacitance C and the current flowing through the arc channel, respectively.

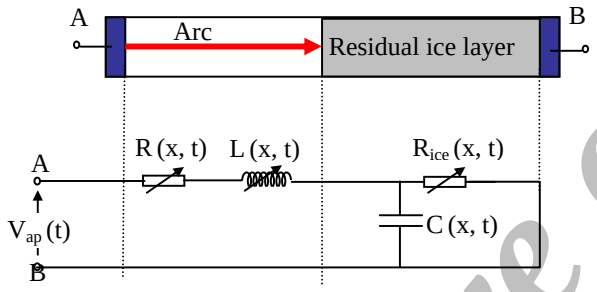

Figure 12: Modeling principle of the arc propagating on the ice-covered surface.

The arc channel resistance, R_{arc}, is obtained from energy balance equations [23, 45]. In order to derive an expression of the relationship between the electrical conductivity of the channel and the electrical characteristics of the circuit, it is assumed that the discharge occurs in a time so short that radiation and heat loss by conduction are negligible. The arc channel resistance is calculated dynamically using the following equation [23, 45]:

$$R_{arc} = \frac{cx}{I_{arc} t^{0.6}} \quad (8)$$

where x is the channel length and where the constant c depends on the voltage type.

The arc channel root radius r (in cm), can be calculated according to Wilkins empirical model [47]:

$$r(t) = \sqrt{\frac{I_{arc}(t)}{k\pi}} \quad (9)$$

where k = 0.875 for AC voltage [15].

In order to determine the inductance of the discharge channel, we used a method similar to that proposed in [26] for discharge in air gaps, where the end effects are ignored and the inductance per unit length of the channel, L_{arc}, is:

$$L_{arc} = \frac{\mu_o}{2\pi}\left[0.25 + \ln\left(\frac{Df}{r}\right)\right] \quad (10)$$

where $\mu_o = 4\pi\ 10^{-7}$ and Df is the distance of the point away from the discharge axis, where the electric field is equal to zero. If Df is large enough for transient fields, the fractional error, which is of the order of 1/ln(Df/r), will be low. For these investigations, we set Df=100m, a typical value already proposed in reference [26].

The capacitance C(x, t) is calculated using a spherical approximation [41], which yields:

$$C(x,t) = \Gamma\varepsilon r\left(1 + \frac{r}{L_f - x}\right) \quad (11)$$

where Γ represents the solid angle between the arc root and the opposite electrode, and where ε is the permittivity of air.

Since ice is generally considered a non-conductive material [34], the resistance of this part is mainly due to a thin water layer at the ice surface. Such a water film results either from the increase in the ambient air temperature or from the thermal exchange between the ice surface and the stabilized arc. The resistance of such a uniform surface is calculated taking into account the insulator geometry and the constriction of current at the arc root (radius=r). The resistance of the insulator with a narrow ice band is given by [15, 43, 48]:

$$R_{ice} = \frac{1}{\pi\gamma_e}\left[\frac{\pi(L_f - x)}{a} + \ln\frac{a}{2\pi r}\right] \quad (12)$$

where γ_e represents the surface conductivity and a stands for the ice layer width which, in the case of a cylindrical configuration, is calculated as:

$$a = \pi\left(\frac{1}{2}D + \varepsilon_{ice}\right) \quad (13)$$

where D and ε_{ice} are the insulator diameter and ice thickness respectively.

In some previous investigations [4, 15], surface conductivity has been empirically determined as a function of freezing water conductivity, σ_w, at 20°C, as:

$$\gamma_e(\mu s) = \alpha\sigma_w(\mu s/cm) + \beta \quad (14)$$

where α = 0.0675 and β=2.45.

Although many mechanisms have been suggested over the years to account for arc motion, mostly over contaminated surfaces, very little information is available on arc velocity. A review of some proposed models can be found in [48, 49]. A velocity model has been proposed for discharge in long air gaps [27], and used by Dhabi *et al.* [50] on polluted surfaces. On the other hand, Sundararajan *et al.* proposed a velocity

model based on the electron mobility concept [51]. Various simulations have, however, shown that the formulation proposed by Les Renardières group [27] is in good agreement with experimental data. These authors postulate that the propagation velocity is proportional to the discharge current [27]:

$$v(t) = \frac{I_{arc}(t)}{q_L} \quad (15)$$

where q_L can be considered practically constant.

$$q_L = \frac{1}{x}\int_0^t I_{arc}(t) \quad (16)$$

During each iteration, after the calculation of the circuit parameters, if an appropriate criteria is met, the arc will expand to a new length (i.e. x = x + v(t)dt). To achieve the minimum critical flashover voltage, the Wilkins' propagation criterion [47] was used:

$$dP_{arc}/dx > 0 \quad (17)$$

where P_{arc} represents the power supplied to the arc by the power source.

4.3. Results and validations

The mathematical dynamic model developed was validated using an insulator string of 5 IEEE standard units (see Fig. 13) covered with artificial ice.

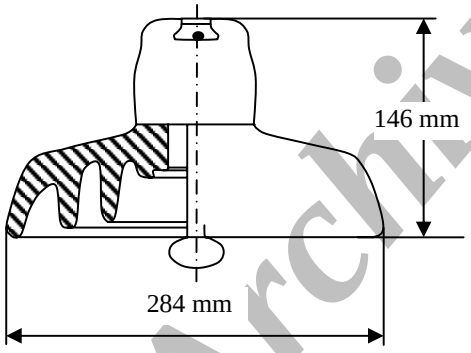

Figure 13: IEEE standard insulator unit.

Up to date, no standard method for evaluating the withstand voltage of insulators under ice and snow conditions has been devised. The development of testing methods for evaluating HV insulator flashover voltage under icing conditions is still at an early stage. Recently, test methods for evaluating flashover voltage of ceramic and non-ceramic insulators under ice, snow, and cold-fog conditions were recommended [7]. Considering that each test nearly takes one full day, it was proposed that the maximum withstand voltage method was more practical for evaluating the performance of iced insulators. A detailed description of this method was presented in our previous studies [7, 9]. Maximum withstand voltage, V_{WS}, is considered to be the maximum voltage at which flashover does not occur in at least three tests out of four.

Artificial ice was deposited at -12°C on a short string of 5 IEEE insulator units, suspended vertically in the center of the climate room (Figure 14).

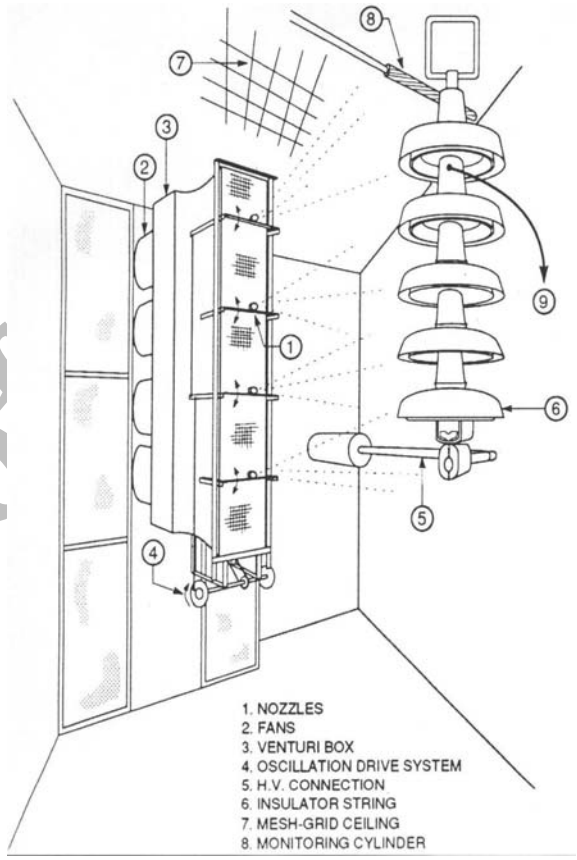

Figure14: Climate room and facilities at the CIGELE laboratories.

Super-cooled droplets having a mean diameter of 80μm, were produced by five pneumatic nozzles at a wind velocity of 3.3m.s^{-1}. Water with a mean conductivity of 80μS/cm, was used to feed the nozzles. The ice deposited under the above conditions was glaze with a density of 0.87g.cm^{-3}. It should be noted that this kind of ice is the most severe type associated to the flashovers on ice-covered insulators [4, 7]. Ice thickness on the monitoring cylinder was 15 mm.

AC high voltage was supplied to the insulator string by a 240kVA, 120kV transformer with a 240kV regulator (Figure 15). The overall short-circuit current of the HV system is about 28A at the maximum

operating voltage of 120kV rms. The insulator leakage current and the voltage were measured using a LabVIEW® data acquisition system.

Different arcing distances *Lf*, varied from 20 to 100cm and a freezing water conductivity σ=80μS/cm was used in these experiments. The initial values of the arc resistance and length were set to 2000Ω/cm and 15% of total length respectively. In equation (8), c was set to 5.87 for the propagation of the arc on the short iced insulator surface.

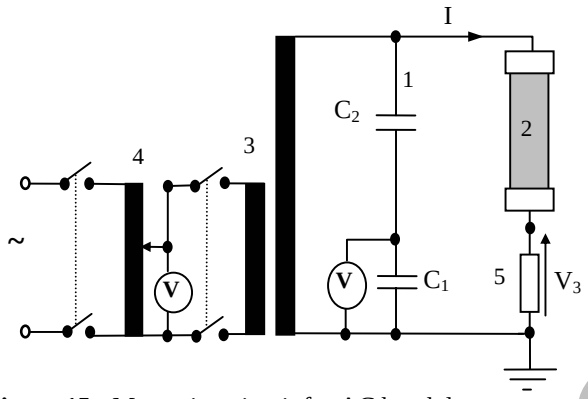

Figure 15: Measuring circuit for AC breakdown test.

Figures 16 and 17 show typical variations in leakage current for two cases of withstand and flashover.

It may be seen that in the flashover case, leakage current increased up to several mA in a very short period and then suddenly increased.

Figures 16b and 17b show the calculated leakage current using the mathematical model developed.

The simulated and measured leakage current waveforms are similar except for the high-frequency noise on the measured currents.

Figure 18 compares the measured and calculated maximum withstand voltages, V_{ws}, of the 5-unit string of IEEE standard insulators covered with glaze. It may be seen that there is good concordance between the flashover values calculated from the model and the experimental results obtained in laboratory. The maximum errors are ~7%.

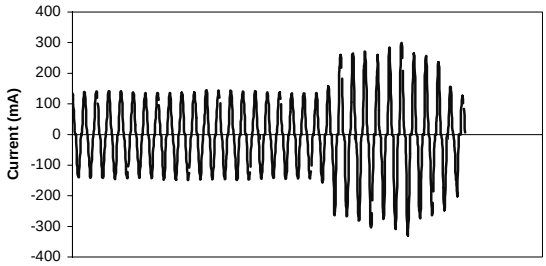

(a)

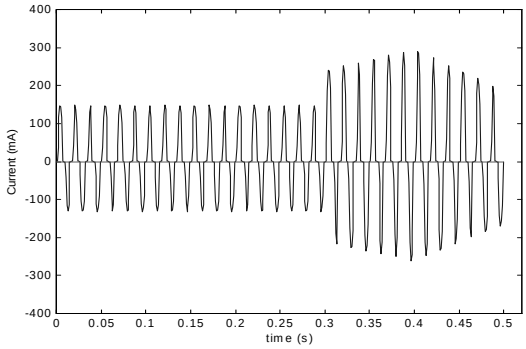

(b)

Figure 16: Typical waveform of the leakage current for a withstand case (a): Measured (b): Simulated.

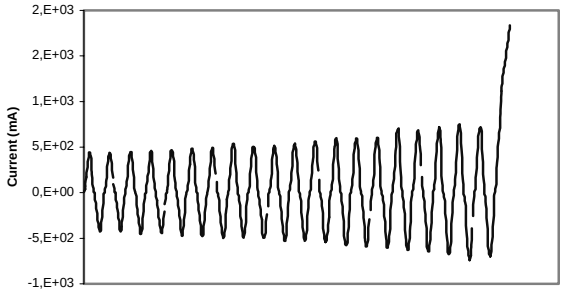

(a)

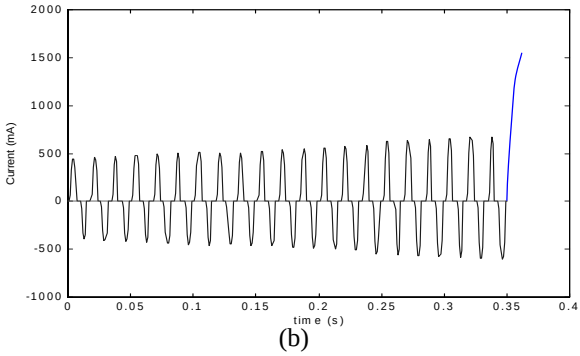

(b)

Figure 17: Typical waveform of the leakage current for a flashover case (a): Measured (b): Simulated.

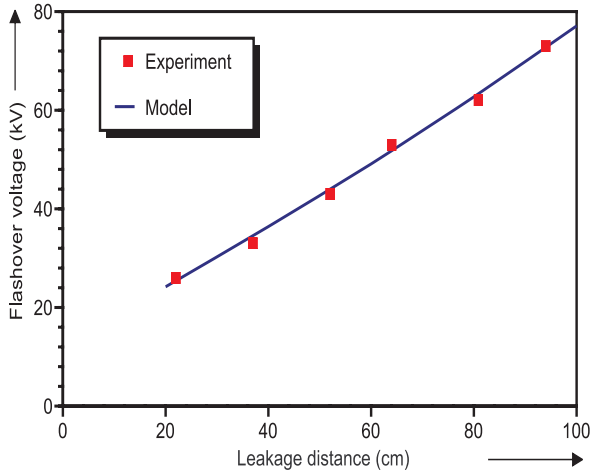

Figure 18: Comparison between the V_{WS} measured under AC and those computed from the model.

5. Conclusions

Experiments were carried out on an ice surface to investigate the mechanisms of corona streamer inception and propagation. Interpretation was helped by comparison with parallel experiments in an air gap, using identical electrodes.

Based on elements derived from physical analysis and interpretation, some empirical equations for the corona streamer inception field and propagation velocity on an ice surface were proposed. The proposed empirical equations, taking in account freezing water conductivity, HV electrode radius, and inception voltage, could be useful to solve practical problems. However, further improvements should be made by taking into account the influence of inter-electrode distance and surrounding air temperature.

Furthermore, the feasibility of using a dynamic arc modeling of iced insulators to predict AC flashover has been presented. The proposed mathematical model is based on a simplified simulation of the successive phases of flashover development process on ice-covered insulators. The flashover voltages calculated from the model were compared to those obtained experimentally on a 5-unit IEEE standard insulator string covered with ice. There was good agreement between the measured and calculated values of maximum withstand flashover voltage.

6. Acknowledgments

This research project was carried out within the framework of the NSERC/Hydro-Quebec/UQAC Industrial Chair on Atmospheric Icing of Power Network Equipment (CIGELE), as well as the Canada Research Chair, tier 1, on Engineering of Power Network Atmospheric Icing (INGIVRE) at Université du Québec à Chicoutimi. The authors wish to thank all the sponsors of the project.

References

[1] "Le grand défi du verglas", CHOC – Magazine de l'Association de l'industrie électrique du Québec, Vol. 20, No. 3, février 2003, p.26.

[2] M. Yasui, K. Naito and Y. Hasegawa, "AC withstand voltage characteristics of insulator string covered with snow", *IEEE Trans. on Power Delivery*, 3(2), 1988.

[3] T. Fujimura, K. Naito, Y. Hasegawa and K. Kawaguchi, "Performance of insulators covered with snow", *IEEE Trans. on Power Apparatus & Systems*, 98, 1979, 1621-1631.

[4] M. Farzaneh, "Ice accretion on high voltage conductors and insulators and related phenomena", *Phil. Trans. of the Royal Soc*. 358(1776), 2000, 2971-3005.

[5] CIGRE Task Force 33.04.09, "Influence of ice and snow on the flashover performance of outdoor insulators, part I: Effects of Ice", *Electra*, 187, 1999, 91-111.

[6] CIGRE Task Force 33.04.09, "Influence of ice and snow on the flashover performance of outdoor insulators, part II: Effects of Snow", *Electra*, 188, 55-69, 2000.

[7] M. Farzaneh et al. "Insulator Icing Test Methods and Procedures" A position paper prepared by the IEEE Task Force on Insulator Icing Test Methods, *IEEE Trans. on Power Delivery*, Vol. 18, No. 4, octobre 2003, pp. 1503-1515.

[8] M. Farzaneh, J. Kiernicki and J. F. Drapeau "AC Flashover performance of HV insulators under Glaze and Rime", *in Proc. 1993 IEEE Conference on Electrical Insulation and Dielectric Phenomena* 93CH3296-8, pp. 499–507, Pocono Manor, October 1993.

[9] M. Farzaneh and J. Kiernicki "Flashover performance of IEEE standard Insulators under ice conditions", *IEEE Electrical Insulation Magazine*, vol. 11, No 2, pp. 5-17, March/April 1995.

[10] M. Farzaneh and J. Kiernicki "Flashover problems caused by ice build-up on Insulators", *IEEE*

Trans. on Power Delivery, vol. 12, No. 4, pp. 1602-1613, 1997.

[11] M. Farzaneh, J.F. Drapeau: "AC Flashover Performance of Insulators Covered with Artificial Ice", IEEE Trans. on Power Delivery, Vol. 10, No. 2, 1995, pp. 1038-1051.

[12] N. Sugawara, T. Takayama, K. Hokari, K. Yoshida, S. Ito: "Withstand Voltage and Flashover Performance of Iced Insulators Depending on the Density of Accreted Ice", Proceedings of the 6th International Workshop on Atmospheric Icing of Structures, Budapest, Hungary, 1993, pp. 231-235.

[13] M. Farzaneh, O.T. Melo: "Flashover Performance of Insulators in the Presence of Short Icicles", International Journal of Offshore and Polar Engineering, Vol. 4, No. 2, 1994, pp. 112-118.

[14] M. Farzaneh, J. Zhang and X. Chen "Variation of Ice Surface Conductivity during Flashover", *IEEE CEIDP*, pp. 631-638, Arlington, TX. 1994.

[15] J. Zhang and M. Farzaneh: "Propagation of AC and DC Arcs on Ice Surfaces", *IEEE Trans. on Diel. and Elec. Insul.*, 7(2), 2000, 269-276.

[16] C. L. Phan and H. Matsuo, "Minimum flashover voltage of iced-insulators", *IEEE Trans. on Elec. Insul.*, vol. 18, No 6, pp. 605-618, 1983.

[17] C. Volat, M. Farzaneh and A. Gakwaya, "Voltage and Field Distribution around a Post Insulator Covered with Atmospheric Ice". The Proceedings of the 9th International Workshop on Atmospheric Icing of Structures, session 4b, Chester, United Kingdom, June 2000.

[18] M. F. Hoyaux "Arc Physics" Srpinger-Verlag New York inc, 1968.

[19] M. Akyuz, L. Gao, V. Cooray, T. G. Gustavsson, S. M. Gubanski and A. Larsson, Positive streamer discharge along insulating surface. *IEEE Trans. on Diel. and Elec. Insul.*, 8(6), 2001, 902-910.

[20] N. L. Allen and B. H. Tan, "Initiation of positive corona on insulator surface". *Proc. of the 12th Int. Symp. on High-Voltage Engineering (ISH)*, Bangalore, India, Vol. 3, August 2001, paper 5-18.

[21] I. Gallimbertti, I. Marchesi and L. Niemeyer, "Streamer corona at an insulating surface". *Proc. 7th Int. Symp. on High Voltage Engineering*, Dresden (Germany), August 1991, paper 41.10.

[22] T. S. Sudarsham and R. Dougal, "Mechanisms of surface flashover along solid dielectrics in compressed gases, a review". *IEEE Trans. on Elec. Insul.*, 21, 1986, 727-746.

[23] J. M. Meek and J. D. Graggs, *Electrical Breakdown of gases*, John Wiley and Sons, New York, 1978.

[24] G. Le Roy, C. Gary, B. Hutzler, J. Lalot, C. Dubanton, "Les propriétés diélectriques de l'air et les très hautes tensions", Éditions Eyrolles, Paris, 1984.

[25] N. St J. Braithwaite, "Introduction to gas discharges". *Plasma Sources Sci. Technol.*, 9, 2000, 517-527.

[26] I. Fofana and A. Béroual, "A predictive model of the positive discharge in long air gaps under pure and oscillating impulse shapes". *J. Phys. D: Appl. Phys.*, 30, 1997, 1653-1667.

[27] Les Renardières Group, "Positive discharges in long air gaps at les Renardières". *Electra*, 53, 1977, 31-153.

[28] M. Farzaneh, I. Fofana, I. Ndiaye, C. Volat and K. D. Srivastava, "Corona Streamer Inception at an Ice Surface" *2nd IASTED Int. Conf. on Power and Energy Systems*, Crete, Greece, June 23 - 26th 2002.

[29] I. Ndiaye, I. Fofana and M. Farzaneh, "Contribution à l'Étude de l'Initiation des Décharges Électriques à la Surface de Glace", *Canadian Conference on Electrical and Computer Engineering*, Montreal (Qc, Canada) May 4-7th 2003.

[30] M. Farzaneh, I. Fofana, I. Ndiaye and K. D. Srivastava, "Experimental studies of Ice Surface discharge Inception and development", International Journal of Power and Energy Systems (accepted).

[31] M. Farzaneh and I. Fofana, "Experimental Study and Analysis of Corona Discharge Parameters on an Ice Surface", Journal of Physics D: Applied Physics (accepted).

[32] Vlad Sadtchenko and George E. Ewing, "A new approach to the study of interfacial melting of ice: infrared spectroscopy", Can. J. Phys. 81: 333–341 (2003).

[33] J. S. Wettlaufer, "Ice surfaces: macroscopic

effects of microscopic structure", Phil. Trans. R. Soc. Lond. A (1999) **357**, 3403–3425.
P. V. Hobbs, *Ice Physics*, Clarendon Press, Oxford, 1974.

[34] R. D. Lide and H. P. R. Frederikse, *Handbook of Chemistry and Physics, 77th Ed.* CRC Press, 1996.

[35] Y. Teyssere and M. Farzaneh, "On the mechanisms of the ice accretion on H.V. conductors", Cold Regions Science and Technology, Vol. 18, pp 1-8, 1990.

[36] M. Frazaneh, S. Li and K. D. Srivastava, "Flashover Process along Ice Surfaces". Atmospheric Research, Elsevier, Les Pays-Bas, Vol. 46, May 1998, pp. 37-47.

[37] S. Brettschneider, M. Farzaneh and K.D. Srivastava, "Ice Surface Discharge Initiation", Power Engineering Review, Vol. 22, No. 8, August 2002, pp. 59-60.

[38] M. Chiba, A. Kumada and K. Hidaka, "Inception Voltage of Positive streamer and its length on PMMA in Air", IEEE Trans. on Diel. and Elec. Insul. 9(1), 2002 118-123.

[39] N L Allen and A A R. Hashem, "The role of negative ions in the propagation of discharges across insulating surfaces", J. Phys. D: Appl. Phys. 35(2002) 2551–2557.

[40] I. Fofana and A. Beroual, "Pre-discharge Models of Dielectric Liquids" *Japanese Journal of Applied Physics*, 37(5A), Part 1, 1998, 2540-2547.

[41] I. Fofana and A. Beroual, "A new proposal for calculation of the leader Velocity based on energy considerations" *J. Phys. D: Appl. Phys.*, 29(3), 1996 691-696.

[42] M. Farzaneh, I. Fofana, C. Tavakoli and X. Chen, "Dynamic Modelling of DC Arc Discharge on Ice Surfaces", *IEEE Trans. on Diel. and Elec. Insul.* 10(3), 2003, 463-474.

[43] M. Farzaneh and J. Zhang, "Modelling of DC arc discharge on ice surfaces", *IEE Proc.-Gener. Trans. Distrib., Vol. 147, No. 2*, pp. 81-86, 2000.

[44] I. Fofana, C. Tavakoli and M. Farzaneh, "Dynamic Modelling of AC Iced Insulator Characteristics", paper 380, *IEEE Power Tech, Bologna (Italy)*, June 23-26 2003.

[45] F. Obenaus, "Fremdschichtüberschlag und Kriechweglänge", *Deutsche Elektrotechnik*, 4, 1958, 135-136.

[46] R. Wilkins, "Flashover voltage of HV insulators with uniform surface pollution films, *Proc. IEE*, 116(3), 1969, 457-465.

[47] F. A. M. Rizk, "Mathematical models for pollution flashover". *Electra*, 78, 1981, 71-103.

[48] I. Fofana, M. Farzaneh and C. Tavakoli, "*Modeling Arc Propagation Velocity on Ice-covered Surfaces*", *The 10th International Workshop on Atmospheric Icing of Structures*, Brno, Czech Republic, June 17-20th 2002.

[49] N. Dhabi-Megriche and A. Beroual "Flashover Dynamic Model of Polluted Insulators under ac Voltage", *IEEE Trans. on Diel. And Elec. Insul.*, 7(2), 2000, 283-289.

[50] R. Sundararajan and R. S. Gorur, "Dynamic arc Modeling of pollution flashover of insulators under DC voltage", IEEE Trans. on Elec. Insul. 28(2), 1993, 209-217.